ELSEVIER

Biochimica et Biophysica Acta 1204 (1994) 225–234

BBA Biochimica et Biophysica Acta

Fluorescence dynamics of staphylococcal nuclease in aqueous solution and reversed micelles

A.J.W.G. Visser [a,*], J. van Engelen [a], N.V. Visser [a], A. van Hoek [b], R. Hilhorst [a], R.B. Freedman [c]

[a] *Department of Biochemistry, Agricultural University, Dreijenlaan 3, 6703 HA Wageningen, The Netherlands*
[b] *Department of Molecular Physics, Agricultural University, 6703 HA Wageningen, The Netherlands*
[c] *Biological Laboratory, University of Kent, Canterbury, Kent CT2 7NJ, UK*

(Received 8 October 1993)

Abstract

The dynamical fluorescence properties of the sole tryptophan residue (Trp-140) in *Staphylococcus aureus* nuclease (EC 3.1.31.1) have been investigated in aqueous solution and reversed micelles composed of either sodium bis(2-ethylhexyl)sulfosuccinate (AOT) in isooctane or cetyltrimethylammonium chloride (CTAC) in isooctane/hexanol (12:1 by volume). The fluorescence decay of nuclease in the different environments can be described by a trimodal distribution of fluorescence lifetimes at approx. 0.5, 1.5 and 5.0 ns. The relative amplitudes depend on the environment. For pH 9.0 solutions the contribution of the two shortest lifetime components in the distribution is largest for AOT and smallest for CTAC reversed micelles. There is reasonable agreement between the average fluorescence lifetime and the fluorescence quantum efficiency confirming a significant fluorescence quenching in AOT reversed micelles. Fluorescence anisotropy decay revealed that the tryptophan environment in aqueous nuclease solutions is rigid on a nanosecond timescale. When nuclease was entrapped into reversed micelles the tryptophan gained some internal flexibility as judged from the distinct presence of a shorter correlation time. The longer correlation time reflected the rotational properties of the protein-micellar system. Modulation of the overall charge of nuclease (isoelectric point pH 9.6) by using buffer of pH 9.0 and pH 10.4, respectively, and of the size of empty micelles by selecting two values of the water to surfactant molar ratio, had only a minor effect on the rotational properties of nuclease in the positively charged reversed micelles. Encapsulation of nuclease in anionic reversed micelles resulted in the development of protein bound to aggregated structures which are immobilised on a nanosecond timescale. According to far UV circular dichroism results the secondary structure of nuclease only followed the already published pH-dependent changes. Encapsulation had no major effect on the overall secondary structure.

Key words: Reversed micelle; Fluorescence anisotropy; Maximum entropy method; Lifetime distribution; Correlation time distribution

1. Introduction

Thermodynamically stable, optically transparent, reversed micelles have been utilised as an important tool in the field of micellar enzymology [1–3]. The popularity stems from the fact that micelle encapsulated enzymes retain their catalytic activity. Furthermore, these media have the additional advantage that the water content, and therefore the protein hydration level, can be controlled through the parameter w_0, which is the water to surfactant molar ratio [4]. It is not only the water content that determines the catalytic properties but also the overall charge of the protein and the charge of the surfactant molecules making up the reversed micelles [5,6]. In order to obtain a detailed insight into these factors and their fine tuning, one should employ methods that are able to probe protein-surfactant interactions at a molecular level.

* Corresponding author. Fax: +31 8370 84801.

Abbreviations: AMPSO, 3-[dimethyl(hydroxymethyl)methylamino]-2-hydroxypropanesulfonic acid; AOT, sodium bis(2-ethylhexyl)-sulfosuccinate; CAPS, 3-[cyclohexylamino]-1-propanesulfonic acid; CD, circular dichroism; CTAB, cetyltrimethylammonium bromide; CTAC, cetyltrimethylammonium chloride; DCM, 4-dicyanomethylene-2-methyl-6-(*p*-dimethylaminostyryl)-4H-pyran; MEM, maximum entropy method

SSDI 0167-4838(93)E0199-C

The methods of choice comprise spectroscopic techniques (reviewed in [7]), but only a few of these contain sufficient sensitivity and molecular resolution to probe these interactions. From scattering techniques conclusions can be drawn regarding gross morphological changes in reversed micelle-protein structures [8]. Nuclear magnetic resonance has the potential to yield information in molecular detail, but the method is hampered by the large concentrations of protein needed to obtain good spectra. From the point of view of surfactants the concentration forms no bottleneck to acquire good quality NMR spectra [9]. Similar arguments apply for a technique as circular dichroism, which is widely applied to reveal secondary structure of proteins. Since the spectra have to be obtained in the far UV, where there is strong light absorption of surfactant, extra care has to be taken to make this method of practical use [3,10]. Several sensitive probe techniques are available to monitor the dynamics of protein-surfactant interaction in reversed micelles: fluorescence recovery after photobleaching [11] and time-resolved fluorescence anisotropy [10,12,13]. Time-resolved fluorescence anisotropy has been brought to a level of considerable sophistication [4,14] and the method provides information not only on overall protein rotation but also on internal motion of fluorescent reporter groups or, when applicable, on energy transfer between identical chromophores.

In order to focus attention to protein-surfactant interaction one should concentrate on a well characterised protein which possesses a single polypeptide chain and preferably one tryptophan residue at known location. Nuclease isolated from *S. aureus* is an example of such a protein. It is a protein of low molecular weight (16807 Da) consisting of a single polypeptide chain with known three-dimensional structure [15,16]. The enzyme catalyses the calcium dependent hydrolysis of RNA or DNA [15]. The gene encoding staphyloccocal nuclease has been cloned into *Escherichia coli* making available large amounts of native and mutant proteins [17,18]. Nuclease contains a single tryptophan residue at position 140 in the sequence, which is remote from the active site. Therefore the enzyme is equipped with a natural fluorescent probe for the observation of protein-surfactant interaction in reversed micelles. An additional advantage is that Trp-140 is held quite rigidly in the protein matrix, a conclusion drawn from fluorescence quenching and steady-state anisotropy results [19]. This study was aimed at measuring the interactions between charged nuclease and two oppositely charged surfactant interfaces in reversed micelles by fluorescence methodologies. The anionic surfactant consisted of AOT and the cationic surfactant of CTAC. The chloride counterion instead of the bromide variant was selected to prevent any quenching by bromide in CTAB reversed micelles. The nuclease has its isoelectric point at pH 9.6 and buffers were chosen such that the overall charge of the protein was either positive (pH 9.0) or negative (pH 10.4). The secondary structure of the protein was checked using far UV circular dichroism.

2. Materials and methods

S. aureus nuclease was prepared from *E. coli* strains as earlier described [17,18]. Its activity in aqueous solution was checked by published procedures [20,21]. Two different buffers were used to dissolve the nuclease: for pH 9.0 50 mM AMPSO (Sigma, St. Louis, MO, USA) and for pH 10.4 50 mM CAPS (Sigma). Reversed micelles were prepared by adding a limited amount of buffer (either 50 mM AMPSO or 50 mM CAPS) to either 0.1 M AOT (50 mM for the CD-experiments) (Fluka, Buchs, Switzerland) dissolved in isooctane or 0.1 M CTAC (Kodak, Rochester, NY, USA) dissolved in isooctane/hexanol mixture (12:1 based on volume, hexanol is also co-surfactant) until the desired w_0 (either 10.6 or 25) was obtained. The mixture was shaken until the solution was clear. Enzyme-containing reversed micellar solutions were similarly prepared by injecting the right volume of buffer and enzyme to the surfactant solution until the desired w_0 was obtained. For both aqueous and reversed micelles the concentration of nuclease was 2.9 μM based on overall volume.

Circular dichroism. CD spectra were recorded between 195 and 240 nm on a Jobin-Yvon Mark V dichrograph in cuvettes of 1 mm path length and analysed for secondary structure using the Contin computer program supplied by Dr. S.W. Provencher (Max Planck Institute, Göttingen, Germany) and described in reference [22]. In case of AOT as surfactant 0.05 M AOT was used as 0.1 M AOT completely blocked the light below 210 nm.

Steady-state fluorescence. Fluorescence spectra were obtained on a SLM-Aminco SPF-500 spectrofluorometer (Urbana, IL, USA) using an excitation wavelength of 295 nm and 4 nm slit widths for both excitation and emission monochromators.

Time-resolved polarised fluorescence. Polarised fluorescence decay curves were measured by the time-correlated single photon counting technique. The excitation source consisted of the frequency-doubled output of a DCM dye laser which was synchronously pumped by a mode-locked argon ion laser (Coherent, Palo Alto, CA, USA). The excitation pulse frequency was reduced to 600 kHz, the pulse duration was less than 4 ps and the excitation light was vertically polarised. Further technical details are given in reference [23]. An excitation wavelength of 303 nm was selected. This wavelength was chosen for red-edge excitation to yield the highest possible initial anisotropy thereby increasing

the dynamic range of the method. Emission was measured through a combination of a WG320 cutoff filter (Schott, Mainz, Germany) and a UG11 broad bandpass filter (Schott). Excitation and detection conditions have been indicated in Fig. 1. The instrumental response function, corresponding to the laser pulse convoluted with the detection response, was determined by measuring the fluorescence decay of an ultrafast decaying pseudoazulene in n-hexane (fluorescent grade, Merck, Damstadt, Germany) having a lifetime of 10 ps [24]. Tryptophan fluorescence in nuclease was sampled during 20 cycles of 10 seconds in each polarisation direction where the detection frequency of the parallel polarised component was set to 30 kHz (5% of 600 kHz) to prevent pulse pile-up. The pseudoazulene reference was sampled during 2 cycles of 10 s in each polarisation direction. Background (same solution but without protein) was usually sampled at one quarter of the sample acquisition time. One complete measurement consisted of measuring the polarised fluorescence decays of the reference compound, the sample, the background and again the reference compound.

All experiments were conducted at 25°C.

Data analysis. Analysis of the total fluorescence decay and fluorescence anisotropy decay $r(t)$ was performed with the commercially available maximum entropy method (MEM, Maximum Entropy Data Consultants, Cambridge, UK). The principle of MEM has been described in the literature [14,25]. For the analysis of the total fluorescence decay of the tryptophan in nuclease into a distribution of lifetimes τ with amplitudes α, 100 equally spaced values on a $\log(\tau)$ scale between 0.01 and 20 ns were used. The starting distribution model was chosen to be flat in $\log(\tau)$ space (all lifetimes have equal probability), since no a priori knowledge about the system was present. The average

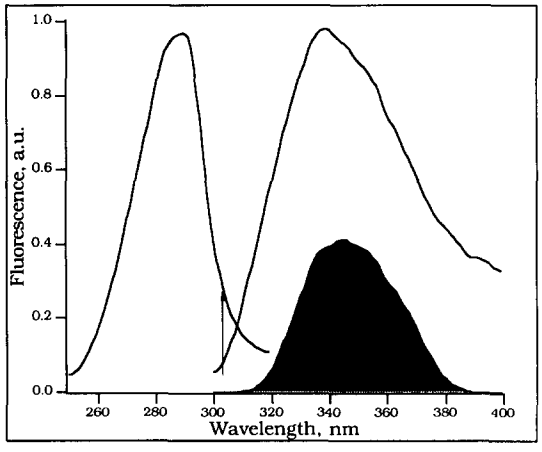

Fig. 1. Excitation and emission spectra of staphylococcal nuclease in CAPS buffer (pH 10.4). The arrow indicates the excitation wavelength and the shaded spectrum is the emission measured through the filter combination used in time-resolved fluorescence experiments.

fluorescence lifetime $\langle\tau\rangle$ can be calculated from the image of the fluorescence lifetime distribution according to:

$$\langle\tau\rangle = \sum_{i=1}^{N} \alpha_i\tau_i \Big/ \sum_{i=1}^{N} \alpha_1 \qquad (1)$$

where N is the number of exponential components in the lifetime distribution ($N = 100$). Similarly, in the (one-dimensional) anisotropy analysis one obtains a spectrum of amplitudes β against correlation times ϕ. In this case, the final image $\alpha(\tau)$ of the fluorescence decay was introduced as a fixed image in the analysis of the anisotropy decay. As a starting model, 100 equally spaced values on a $\log(\phi)$ scale (from 0.1 to 100 ns) were used in the analysis. Similar considerations regarding the starting model in the recovery of $\alpha(\tau)$ apply to the recovery of $\beta(\phi)$, i.e., if one has no *a priori* knowledge of the distribution one should start with a flat spectrum in $\log(\phi)$ space. The integrated amplitude $\beta(\phi)$ corresponds to the initial anisotropy r_0. From time-resolved polarised fluorescence experiments one is also able to recover the complete three-dimensional image which is given by the number of fluorophores with lifetime τ, rotational correlation time ϕ and initial anisotropy r_0 [26]. In all cases studied the χ^2 values were close to 1.0, and, in addition, the weighted residuals between experimental and calculated decay curves and the autocorrelation function of the residuals [27] were randomly distributed around zero indicating an optimal fit to the data. Examples of these fit quality criteria are given in Figs. 2 and 3. Reproducibility was found to be satisfactory in duplicate experiments.

The fluorescence anisotropy decay of tryptophan in proteins can be adequately described by a superposition of two independent motions, namely a rapid internal motion of tryptophan within the protein (characteristic time ϕ_{int}) and the much slower protein rotation (characteristic time ϕ_{prot}):

$$r(t) = \{\beta_1 \exp(-t/\phi_{int}) + \beta_2\} \exp(-t/\phi_{prot}) \qquad (2)$$

When $\phi_{int} \ll \phi_{prot}$ then the short observed correlation time is very close to ϕ_{int}. The preexponential factors are related to the so-called order parameter S for the tryptophan residue, via:

$$S^2 = \beta_2/(\beta_1 + \beta_2) \qquad (3)$$

When there is no internal probe motion ($\beta_1 = 0$), tryptophan rotates together with the whole protein and S is equal to unity. When there is some internal flexibility, the order parameter gives information on the angular displacement ψ, responsible for the rapid internal motion:

$$S^2 = \tfrac{1}{2}\cos\psi(\cos\psi + 1) \qquad (4)$$

From the long correlation time ϕ_{prot} the hydrodynamic radius R_h of the rotating particle (either protein in aqueous solution or the protein-micellar complex as a whole) can be calculated using the Stokes–Einstein equation:

$$\phi_{prot} = \eta V/(kT) = 4\pi R_h^3 \eta/(3kT) \quad (5)$$

where η is the viscosity of the medium (0.890 mPa s for water, 0.474 mPa s for isooctane and 0.50 mPa s for isooctane/hexanol mixture [12] at 25°C), V is the volume, k the Boltzmann constant and T the temperature in K.

4. Results and discussion

Fluorescence and dynamical properties of nuclease in aqueous solution

From the spectral distribution of nuclease fluorescence one can determine the center of gravity of the band [28]. These values obtained for aqueous enzyme solution at pH 9.0 and pH 10.4 are listed in Table 1. The spectral band positions are not essentially different from those reported [19]. The fluorescence intensity integrated over the band is related to the fluorescence efficiency. The efficiency obtained for the nuclease at pH 9.0 was arbitrarily set to 1.0 and fluorescence efficiencies of other nuclease samples were related to it. In this way one can compare relative steady-state fluorescence changes with those of average lifetimes (see below). It is noted that there is a quenching effect visible at pH 10.4 as compared to the data at pH 9.0.

The experimental fluorescence decay of nuclease at pH 9.0 is shown in Fig. 2 together with the MEM

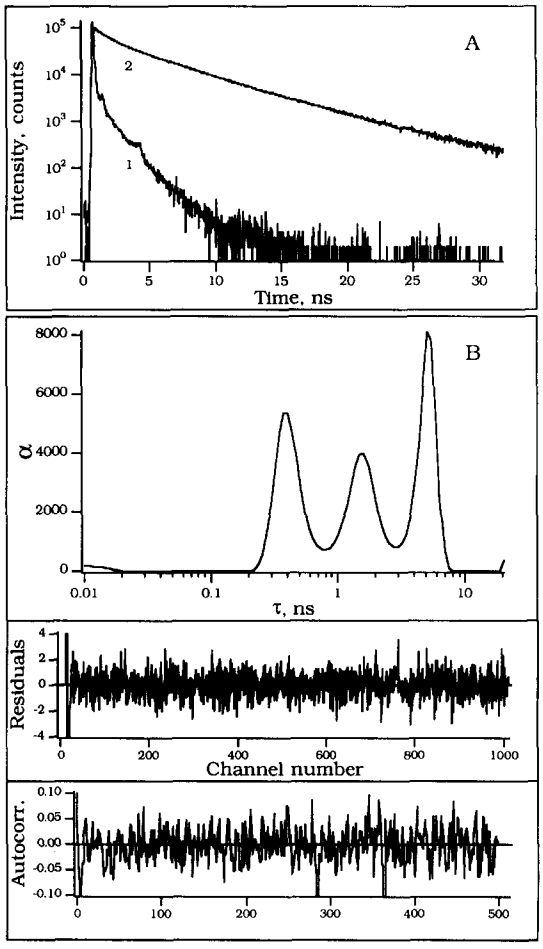

Fig. 2. Fluorescence decay of staphylococcal nuclease in AMPSO buffer (pH 9.0) and maximum entropy analysis into distribution of fluorescence lifetimes. (A) Impulse response function measured via pseudoazulene (1) and experimental total fluorescence decay (2). (B) Fluorescence lifetime distribution ($\alpha(\tau)$) versus τ) with weighted residuals between experimental and fitted curves and autocorrelation function of the residuals ($\chi^2 = 1.14$).

Table 1
Fluorescence parameters of tryptophan in staphylococcal nuclease in aqueous solution and reversed micelles

Solution conditions	λ_{cg} [a] (nm)	q_{rel} [b] (–)	$\langle\tau\rangle$ [c] (ns)
Aqueous buffer			
pH 9.0	333	1	2.5
pH 10.4	338	0.70	1.4
CTAC reversed micelles			
pH 9.0, $w_0 = 10.6$	337	1.38	2.6
pH 9.0, $w_0 = 25$	338	1.25	3.4
pH 10.4, $w_0 = 10.6$	338	1.60	3.6
pH 10.4, $w_0 = 25$	339	1.39	3.4
AOT reversed micelles			
pH 9.0, $w_0 = 10.6$	334	0.59	1.6
pH 9.0, $w_0 = 25$	337	0.45	1.1
pH 10.4, $w_0 = 10.6$	334	0.52	1.1
pH 10.4, $w_0 = 25$	341	0.45	1.2

[a] Center of gravity of fluorescence spectra.
[b] Relative fluorescence efficiency.
[c] Average fluorescence lifetime (Eq. (1)).

analysis in a lifetime distribution. It is clear that a trimodal distribution is the best fit to the data and the barycenters are located at 0.42, 1.57 and 4.91 ns. This heterogeneity in lifetimes had already been observed as a biexponential fluorescence decay by Brochon et al. [29]. It is difficult to trace down the origin of the heterogeneous decay behaviour taking into account that the fluorescence decay of free tryptophan or tryptophanyl derivatives show similar heterogeneity [30,31]. Nuclease forms no exception to the rule that single-tryptophan containing proteins show clear deviation from monoexponentiality of the fluorescence decay [32]. The average fluorescence lifetime is listed in Table 1. The analysis of the fluorescence decay of nuclease at pH 10.4 resulted in a similar trimodal distribution pattern but with larger amplitudes in the shorter lifetime peaks (data not shown). The average lifetime is therefore shorter for the protein at pH 10.4, which is in

keeping with the steady-state fluorescence results (Table 1).

The two polarised (parallel and perpendicular) fluorescence decay curves of nuclease at pH 9.0 are presented in Fig. 3 together with the (global) analysis in a distribution of correlation times using MEM. The correlation time distribution clearly shows a narrow, single peak at 11.6 ns (half width 1.1 ns) and a minor component at 0.2 ns. In Fig. 3 the correlation time distribution of nuclease at pH 10.4 is also given for comparison to illustrate that the protein correlation time is about the same as at pH 9.0 and that a significant contribution of some ultrarapid tryptophan segmental motion can be discerned. The observed longer correlation time is in excellent agreement with the indirectly determined rotational correlation times found previously, namely 10.5 ns [33] and 11.05 ns at 20°C [19]. In Table 2 we have collected all the parameters that can be obtained from the anisotropy data (see Section 2). From a correlation time of 11.6 ns a protein hydrodynamic radius $R_h = 2.3$ nm can be derived using Eq. (5).

When this work was in progress, a report appeared in the literature dealing with the pH-induced unfolding of staphylococcal nuclease using Trp-140 fluorescence changes and far UV circular dichroism [34]. It was found that the midpoint for alkaline unfolding was at pH 10.5, close to our used pH 10.4. This midpoint was obtained by quenching of Trp-140 fluorescence up to 50% of the fluorescence value at pH 7.0. In our experiments we found indeed fluorescence quenching (both intensity and lifetime data, see Table 1). However, if the protein is in an unfolded state one would expect a dramatic increase of the contribution of the short correlation time. There is an increase (see Table 2) but the nuclease at pH 10.4 still rotates as a rather compact globular protein (see Fig. 3). This finding is in agreement with CD data (vide infra). Therefore, direct

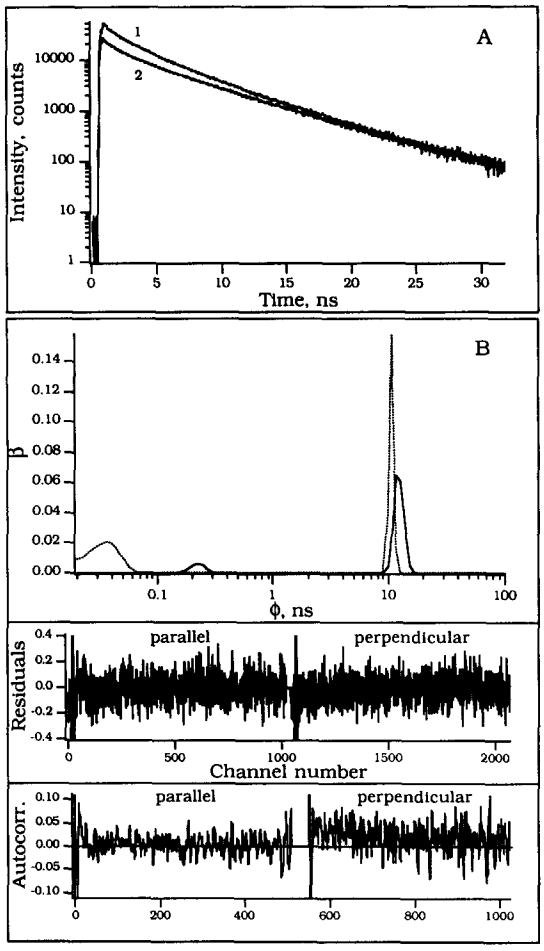

Fig. 3. Polarised fluorescence decay curves of staphylococcal nuclease in AMPSO buffer (pH 9.0) and simultaneous maximum entropy analysis of the two polarised decay curves into a distribution of correlation times. (A) Parallel polarised (1) and perpendicular polarised (2) fluorescence decay curves. (B) Correlation time distribution ($\beta(\phi)$ versus ϕ) pH 9.0 (———), and pH 10.4 (· · · · · ·). Also are shown the residuals and autocorrelation function of the residuals ($\chi^2 = 1.18$).

Table 2
Correlation times and order parameters of tryptophan in staphylococcal nuclease in aqueous solution and in CTAC reversed micelles

Solution conditions	β_1 [a] (–)	ϕ_{int} [b] (ns)	β_2 [a] (–)	ϕ_{prot} [b] (ns)	S [c] (–)	ψ [d] (°)
Aqueous buffer						
pH 9.0	0.026	0.22 (0.03)	0.239	11.6 (1.1)	0.95	23
pH 10.4	0.122	0.04 (0.01)	0.143	10.6 (0.5)	0.73	55
CTAC reversed micelles						
pH 9.0, $w_0 = 10.6$	0.061	0.74 (0.13)	0.204	22.7 (13.8)	0.92	27
pH 9.0, $w_0 = 25$	0.073	1.27 (0.12)	0.192	20.9 (15.0)	0.90	30
pH 10.4, $w_0 = 10.6$	0.058	0.58 (0.08)	0.207	15.7 (6.4)	0.92	26
pH 10.4, $w_0 = 25$	0.100	1.36 (0.26)	0.165	14.0 (3.0)	0.85	36

[a] Determined from integrated curves of correlation time distributions.
[b] Determined from the barycenter and Eq. (2); values in parentheses are the half widths.
[c] Determined from Eq. (3).
[d] Determined from Eq. (4).

monitoring the local flexibility of Trp-140 in denaturation studies seems to be a more powerful method than a steady state spectroscopic one which registers gross conformational changes.

Fluorescence and dynamical properties of nuclease in CTAC reversed micelles

The steady-state fluorescence data indicate fluorescence enhancement when nuclease was incorporated in CTAC reversed micelles (Table 1). The fluorescence lifetime distributions of nuclease in CTAC reversed micelles were again trimodal, independent of either w_0 or pH, with most intensity in the longer components (results not shown). Consequently, the average fluorescence lifetime is longer than in aqueous solution at pH 9.0 (Table 1), in agreement with the increased fluorescence intensity.

In Fig. 4 we have presented the correlation-time distribution for the four different nuclease-CTAC samples (pH 9.0 and 10.4; $w_0 = 10.6$ and 25). Two distinct distributions can be seen, the barycenters are given in Table 2. The shorter correlation times have typical values around 1 ns and must be ascribed to segmental motion of the tryptophan residue. Its contribution has increased as compared to that in aqueous solution (pH 9.0) and therefore the order parameter is less and the angular motional freedom larger (Table 2). Furthermore, the apparent shift to longer times as compared to the short correlation times in water suggests that the frequency of the segmental motion is less than in water (damping). These data definitely show that the microstructure of the protein near Trp-140 is changed in reversed micelles. From inspection of the longer correlation time distribution (Fig. 4) it is immediately apparent that the distributions are distinctly broader as compared to those in aqueous solution (see half widths in Table 2). This observation is indicative for a heterogeneous population of rotating protein-micelle particles. At $w_0 = 10.6$ the barycenter of the long correlation time distribution is at 23 ns at pH 9.0 (nuclease positively charged) and at 16 ns at pH 10.4 (nuclease negatively charged) (see Table 2). In the small micelles the attractive interactions between protein and interface allows the protein-micelle complex to rotate faster than the less compact complex at pH 9.0. If in first approximation the core radii of empty CTAC micelles are assumed identical to those of empty CTAB micelles, then a $w_0 = 10.6$ would implicate a micellar core radius of 2.0 nm [12]. This radius is slightly smaller than the hydrodynamic protein radius of 2.3 nm and, therefore, the nuclease can only be tightly fitted in the droplet. Surprisingly, when nuclease is encapsulated in reversed micelles with $w_0 = 25$, the longer correlation times show hardly any change in peak location. If again an empty micelle is considered and compared to the CTAB case [12], the core radius of a CTAC micelle would be 3.6 nm, which yields a much larger droplet than protein. The correlation time of such an empty reversed micelle is expected to be 110 ns. If the nuclease is incorporated in such large micelle one would expect to see a tendency of this correlation time in the distribution, e.g., as a gradual shift of the distribution to longer time (Fig. 4). Since this effect is not observed our conclusion must be that the enzyme creates its own micelle in CTAC reverse micelles, irrespective of w_0 or pH. Such conclusion was also reached for α-chymotrypsin in AOT reversed micelles [4]. For clarity we have collected in Table 3 the hydrodynamic radii of nuclease-CTAC micelles for the different w_0 and pH used. The radii were calculated with Eq. (5) and lower and upper boundaries of the radii are given based upon the half width values of the long correlation times (cf. Fig. 4).

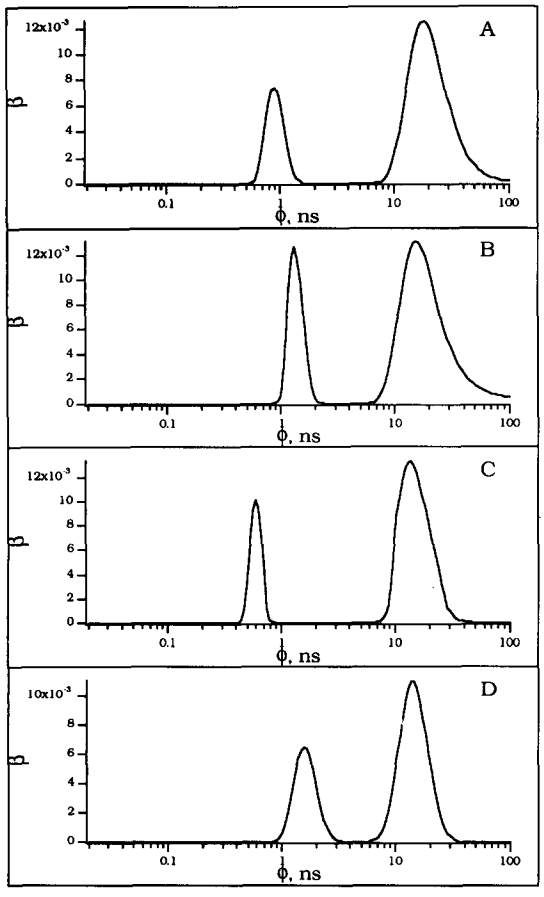

Fig. 4. Distribution of correlation times ($\beta(\phi)$ vs. ϕ) of staphylococcal nuclease in CTAC reversed micelles. (A) pH 9.0 $w_0 = 10.6$; (B) pH 9.0 $w_0 = 25$; (C) pH 10.4 $w_0 = 10.6$; (D) pH 10.4 $w_0 = 25$.

Fluorescence and dynamical properties of nuclease in AOT reversed micelles

When nuclease was encapsulated in AOT reversed micelles, the fluorescence intensity dropped and the average lifetime became shorter (Table 1). The fluores-

Table 3
Hydrodynamic radii of staphyloccocal nuclease-CTAC reversed micelles

Solution conditions	lower bound R_h [a] (nm)	R_h [a] (nm)	upper bound R_h [a] (nm)
pH 9.0, $w_0 = 10.6$	2.87	3.54	3.90
pH 9.0, $w_0 = 25$	2.71	3.45	3.68
pH 10.4, $w_0 = 10.6$	2.66	3.14	3.41
pH 10.4, $w_0 = 25$	2.77	3.02	3.41

[a] Determined from ϕ_{prot} values in Table 2, the half width values and Eq. (5); see text for details.

cence lifetime distribution pattern still consisted of three peaks, but the contribution of the shortest lifetime peak was largest (results not shown). These data indicate a drastic effect on the conformation in the vicinity of tryptophan where the protein is perhaps partially unfolded.

This is also reflected in the distribution profiles of the correlation times. The two examples at pH 9.0 are shown in Fig. 5 to illustrate the complexity of the distribution patterns. At $w_0 = 10.6$ (Fig. 5A) the distribution consisted of three parts, a short peak located at $\phi = 1$ ns, a nonresolved distribution increasing between 10 and 100 ns and a limiting anisotropy corresponding to $\phi \rightarrow \infty$ (depicted at $\phi = 100$ ns). At $w_0 = 25$ (Fig. 5B) the distribution even consisted of four parts, two peaks with relatively large contributions located at $\phi = 0.5$ and $\phi = 3.7$ ns, a similar nonresolved distribution between 10 and 100 ns and a limiting anisotropy depicted at $\phi = 100$ ns. The short correlation times

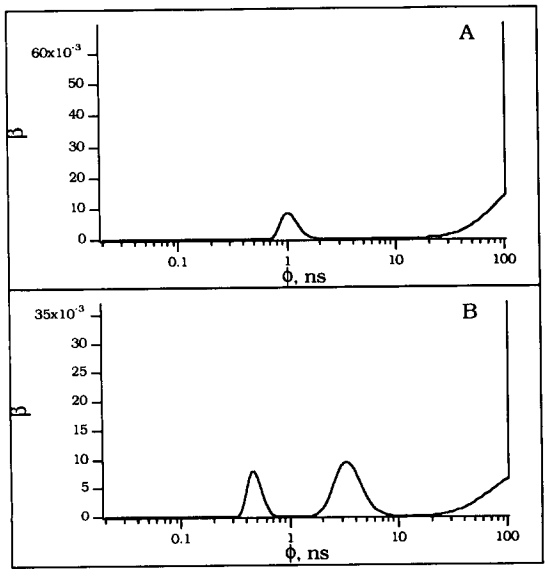

Fig. 5. Distribution of correlation times ($\beta(\phi)$ versus ϕ) of staphylococcal nuclease in AOT reversed micelles at pH 9.0. (A) $w_0 = 10.6$, the limiting anisotropy at $\phi = 100$ ns has a value of 0.069; (B) $w_0 = 25$, the limiting anisotropy at $\phi = 100$ ns has a value of 0.037.

and its relatively large contribution observed at both w_0 values suggest rapid motion of Trp-140 of large angular freedom. The correlation time at 3.7 ns is difficult to assign. It can arise from a population of protein molecules partially surrounded by surfactant molecules and rapidly rotating in the less viscous organic solvent. Alternatively, it can be a slow restricted motion of the protein superimposed on the very slowly rotating aggregate type of motion that is reflected by the nonresolved and infinitely long correlation times. At pH 10.4 similar types of complex distribution patterns can be observed (results not shown). The real nature of these effects on the fluorescence anisotropy would require further investigation.

With AOT reversed micelles it has been demonstrated that proteins like cytochrome *c*, chymotrypsin and ribonuclease at relatively low concentration, promote strong attractive interactions between reversed micelles leading finally to percolation and phase transition [35]. The nuclease concentration used in this work amounted to 2.9 μM on the basis of overall volume (this relatively high concentration was needed because of the red-edge excitation of 303 nm). Conductivity measurements (data not shown) revealed that this concentration is not high enough to induce such a percolation process, so a different explanation for the complex distribution patterns of rotational correlation times must be sought.

Two-dimensional maximum entropy analysis of polarised fluorescence decay

In order to observe whether there is associative behaviour of fluorescence lifetimes and rotational correlation times, we decided to carry out a two-dimensional MEM analysis (the initial anisotropy R_0 was fixed to 0.265) of the polarised fluorescence decay data of nuclease in three different environments (all at pH 9.0). The results are given in Fig. 6 in the form of contour diagrams. From the contour plots of nuclease in aqueous solution (Fig. 6A) it is clear that the shortest lifetime component ($\tau = 0.5$ ns) does not carry information on the anisotropy and thus on the reorientational motion of the protein. One of the points to emphasize in these analyses is the occurrence of so-called 'iso-κ' values which can give rise to artefactual peaks (such an 'iso-κ' solution may arise from the following reciprocal relationships $1/\kappa = 1/\tau_1 + 1/\phi_2 = 1/\tau_2 + 1/\phi_1$) [36]. The information which is contained in the short lifetime peak (0.5 ns) is located on such an 'iso-κ' line. The intermediate lifetime component does not have any bearing on the correlation times. The rotational mobility of the protein is clearly associated with the longest lifetime component ($\tau = 5$ ns) characterised by a dense contour region at $\phi = 4$–12 ns. Similar arguments apply to the results of nuclease in CTAC micelles ($w_0 = 10.6$), in which the longest

lifetime component carries the information on the relatively slow rotation (dense contour levels at $\phi = 10$–20 ns in Fig. 6B). In addition the peaks arising from restricted tryptophan motion at $\phi = 1$ ns are associated with the two longer fluorescence lifetimes. The results obtained with nuclease in AOT reversed micelles ($w_0 = 10.6$) confirmed the complexity of rotational behaviour of Trp-140 in these micelles (Fig. 6C). The short lifetime component ($\tau = 0.6$ ns) does not carry any information on the anisotropy. The intermediate lifetime ($\tau = 2$ ns) is associated with the short correlation time of 1 ns. These results show that there is indeed immobilised protein present, which correlation time cannot be resolved in these experiments. The other two-dimensional analyses of polarised fluorescence decay of the nuclease in AOT reversed micelles yielded similar complex patterns and are not further discussed.

Circular dichroism experiments

CD experiments have been performed in order to determine the overall secondary structure in nuclease

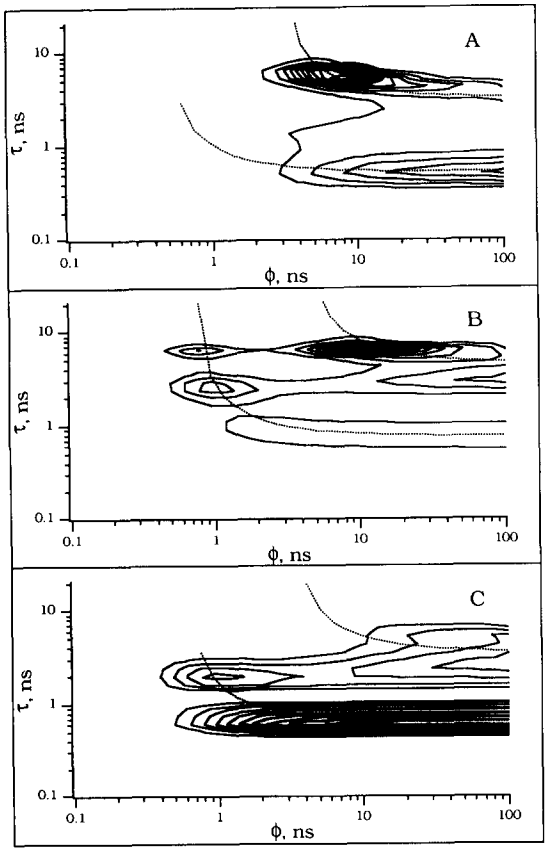

Fig. 6. Contour plot of two-dimensional maximum entropy analysis of polarised fluorescence decay of staphylococcal nuclease. Initial anisotropy R_0 was set at 0.265. The set of hyperbolic curves represents iso-κ values. Details are given in Ref. 26 and in the text. (A) pH 9.0; (B) CTAC reversed micelles, pH 9.0 $w_0 = 10.6$; (C) AOT reversed micelles, pH 9.0 $w_0 = 10.6$.

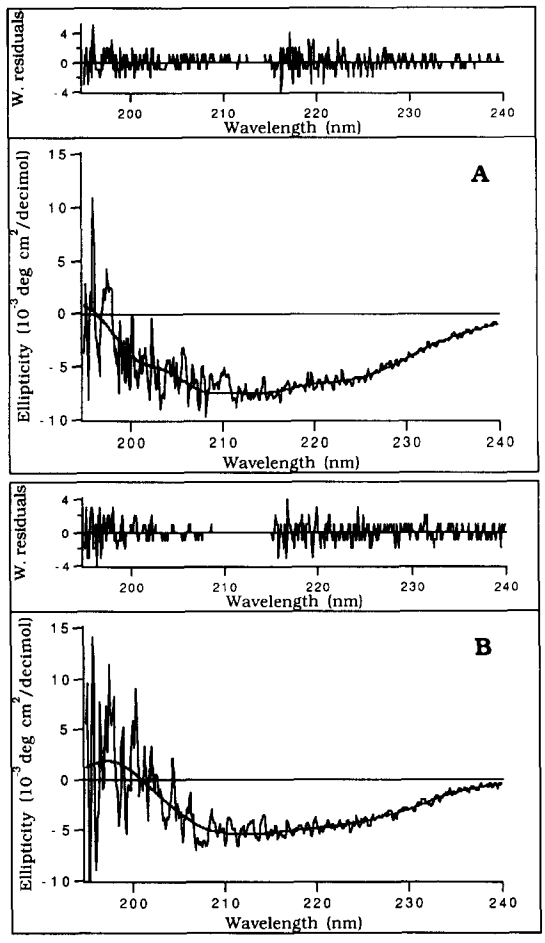

Fig. 7. Experimental and fitted circular dichroism spectra of staphylococcal nuclease in reversed micelles at pH 9.0 and with $w_0 = 25$. The weighted residuals are also shown. The analysis is performed over two separate regions of the spectrum (which is an option provided by the computer program): the noisy spectrum between 195 and 215 nm and the less noisy region between 215 and 240 nm. (A) AOT; (B) CTAC.

when the pH, nature of surfactant and amount of water in the reversed micelles are changed. In Fig. 7 two examples are shown for nuclease in CTAC and AOT reversed micelles and the analysis in secondary structure elements. The spectra are very noisy below 200 nm because of light absorption by the surfactant. The results of the analysis are collected in Table 4. As noted by Chen et al. [34], alkaline denaturation of staphylococcal nuclease is not accompanied by an increase in random structure. The α-helix content decreases upon raising the pH, but a considerable amount of the structure remains β-sheet-like in agreement with the findings of Chen et al. [34]. The situation is unaltered in reversed micelles irrespective of charge of the surfactant or the water content. Therefore we conclude that the polypeptide chain does not undergo drastic changes in secondary structure when the protein is encapsulated. Furthermore the pH-effects on the secondary structure (lowering of α-helix content at

Table 4
Secondary structure content from circular dichroism spectra of staphylococcal nuclease under different solution conditions [a]

Solution conditions	α-Helix (%)	β-Sheet (%)	β-Turn (%)	Random (%)
Aqueous buffer				
pH 7.0	30 (1)	23 (3)	14 (2)	33 (5)
pH 9.0	19 (4)	39 (3)	14 (5)	28 (3)
pH 10.4	8 (3)	41 (2)	18 (3)	33 (6)
CTAC reversed micelles				
pH 9.0, $w_0 = 10.6$	15 (2)	42 (6)	16 (3)	27 (5)
pH 9.0, $w_0 = 25$	13 (1)	39 (2)	21 (1)	27 (1)
pH 10.4, $w_0 = 10.6$	8 (1)	41 (2)	23 (1)	27 (1)
pH 10.4, $w_0 = 25$	9 (2)	45 (3)	20 (1)	26 (1)
AOT reversed micelles				
pH 9.0, $w_0 = 10.6$	20 (3)	42 (4)	12 (3)	26 (3)
pH 9.0, $w_0 = 25$	18 (3)	44 (5)	3 (3)	35 (3)
pH 10.4, $w_0 = 10.6$	8 (1)	48 (2)	20 (1)	24 (1)
pH 10.4, $w_0 = 25$	10 (2)	46 (3)	16 (2)	28 (2)

[a] Values between parentheses are errors resulting from duplicate experiments.

increasing pH) are preserved in reversed micelles. On the basis of these results it can then be concluded that the pH in reversed micelles does not deviate substantially from the bulk buffer pH.

5. Conclusions

Time-resolved polarised fluorescence decay experiments of Trp-140 in staphylococcal nuclease in different media yielded very detailed information on the fluorescence lifetime heterogeneity, the local tryptophan mobility and on the overall protein or protein-micelle motion. Since Trp-140 is rigidly bound in nuclease in aqueous solution, any flexibility induced upon entrapment into reversed micelles may indicate a locally perturbed structure. Based upon the invariant value of the long correlation time the protein seems to create its own micelle irrespective of the water content of the system. Also, the presence of nuclease immobilised onto micellar aggregates can be made visible with this technique. The secondary structure remains largely intact upon encapsulation implying that the tryptophan fluorescence reports only about its own immediate environment.

6. Acknowledgements

The authors thank Dr. C. Oldfield for valuable advice. We also thank Prof. T.Y. Tsong for drawing our attention to the study of the pH-induced unfolding of staphylococcal nuclease. This work was supported in part by NATO Collaborative Research Grant No. 880460.

7. References

[1] Martinek, K., Levashov, A.V., Klyachko, N.L., Khmelnitsky, Y.L. and Berezin, I.V. (1986) Eur. J. Biochem. 155, 453–468.
[2] Luisi, P.L., Giomini, M., Pileni, M.P. and Robinson, B.H. (1988) Biochim. Biophys. Acta 947, 209–246.
[3] Verhaert, R.M.D., Hilhorst, R., Visser, A.J.W.G. and Veeger, C. (1992) in Biomolecules in Organic Solvents (Gomez-Puyou, A., ed.), pp. 133–162, CRC Press, Boca Raton, FL.
[4] Dorovska-Taran, V.N., Veeger, C. and Visser, A.J.W.G. (1993) Eur. J. Biochem. 211, 47–55.
[5] Wolbert, R.B.G., Hilhorst, R., Voskuilen, G., Nachtegaal, H., Dekker, M. and Van 't Riet, K. (1989) Eur. J. Biochem. 184, 627–633.
[6] Hilhorst, R., Verhaert, R.M.D. and Visser, A.J.W.G. (1991) Biochem. Soc. Trans. 19, 666–670.
[7] Vos, K., Laane, C. and Visser, A.J.W.G. (1987) Photochem. Photobiol. 45, 863–878.
[8] Rahaman, R.S. and Hatton, T.A. (1991) J. Phys. Chem. 95, 1799–1811.
[9] Shapiro, Y.E., Budanov, N.A., Levashov, A.V., Klyachko, N.L., Khmelnitsky, Y.L. and Martinek, K. (1989) Collect. Czech. Chem. Commun. 54, 1126–1134.
[10] Gallay, J., Vincent, M., Nicot, C. and Waks, M. (1987) Biochemistry 26, 5738–5747.
[11] Chatenay, D., Urbach, W., Nicot, C., Vacher, M. and Waks, M. (1987) J. Phys. Chem. 91, 2198–2201.
[12] Vos, K., Laane, C., Weijers, S.R., Van Hoek, A., Veeger, C. and Visser, A.J.W.G. (1987) Eur. J. Biochem. 169, 259–268.
[13] Vos, K., Laane, C., Van Hoek, A., Veeger, C. and Visser, A.J.W.G. (1987) Eur. J. Biochem. 169, 275–282.
[14] Bastiaens, P.I.H., Van Hoek, A., Benen, J.A.E., Brochon, J.C. and Visser, A.J.W.G. (1992) Biophys. J. 63, 839–853.
[15] Anfinsen, C.B., Cuatrecasas, P. and Taniuchi, H. (1971) in The Enzymes (Boyer, P., ed.), Vol. 4, pp. 177–199, Academic Press, New York.
[16] Cotton, F.A., Hazen, E.E. and Lego, M.J. (1979) Proc. Natl. Acad. Sci. USA 76, 2551–2555.
[17] Shortle, D.J. (1989) J. Biol. Chem. 264, 5315–5318.
[18] Shortle, D.J. and Meeker, A.J. (1989) Biochemistry 28, 936–944.
[19] Wright, G. and Freedman, R.B. (1989) Protein Eng. 2, 538–588.
[20] Cuatrecasas, P., Fuchs, S. and Anfinsen, C.B. (1967) J. Biol. Chem. 242, 1541–1547.
[21] Cuatrecasas, P., Wilchek, M. and Anfinsen, C.B. (1969) Biochemistry 8, 2277–2284.
[22] Provencher, S.W. and Glockner, J. (1981) Biochemistry 20, 33–37.
[23] Van Hoek, A., Vos, K. and Visser, A.J.W.G. (1987) IEEE J. Quantum Electron. QE-23, 1812–1820.
[24] Visser, A.J.W.G., Kulinski, T. and Van Hoek, A. (1988) J. Mol. Struct. 175, 111–116.
[25] Livesey, A.K. and Brochon, J.C. (1987) Biophys. J. 52, 693–706.
[26] Bastiaens, P.I.H., Van Hoek, A., Brochon, J.C. and Visser, A.J.W.G. (1992) in Time-Resolved Laser Spectroscopy in Biochemistry III (Lakowicz, J.R., ed.), Vol. 1640, pp. 138–147, SPIE, Bellingham, WA.
[27] Vos, K., Van Hoek, A. and Visser, A.J.W.G. (1987) Eur. J. Biochem. 165, 55–63.
[28] Bastiaens, P.I.H., Van Hoek, A., Van Berkel, W.J.H., De Kok, A. and Visser, A.J.W.G. (1992) Biochemistry 31, 7061–7068.
[29] Brochon, J.C., Wahl, Ph. and Auchet, J.C. (1974) Eur. J. Biochem 41, 577–583.
[30] Szabo, A.G. and Rayner, D.M. (1980) J. Am. Chem. Soc. 102, 554–563.
[31] Chang, M.C., Petrich, J.W., McDonald, D.B. and Fleming, G.R. (1983) J. Am. Chem. Soc. 105, 3819–3824.

[32] Beechem, J.M. and Brand, L. (1985) Annu. Rev. Biochem. 54, 43–71.
[33] Lakowicz, J.R., Maliwal, B.P., Cherek, H. and Balter, A. (1983) Biochemistry 22, 1741–1752.
[34] Chen, H.M., You, J.L. and Tsong, T.Y. (1991) J. Mol. Biol. 220, 771–778.
[35] Huruguen, J.P. and Pileni, M.P. (1991) Eur. Biophys. J. 19, 103–107.
[36] Brochon, J.C., Mérola, F. and Livesey, A.K. (1992) in Synchrotron Radiation and Dynamic Phenomena, pp. 435–452, American Institute of Physics, New York.